

Exploitation of Microtubule Cytoskeleton and Dynein during Parvoviral Traffic toward the Nucleus

Sanna Suikkanen, Tuula Aaltonen, Marjukka Nevalainen, Outi Väliilehto,
Laura Lindholm, Matti Vuento, and Maija Viihinen-Ranta*

Department of Biological and Environmental Science, University of Jyväskylä, FIN-40500 Jyväskylä, Finland

Received 21 April 2003/Accepted 30 June 2003

Canine parvovirus (CPV), a model virus for the study of parvoviral entry, enters host cells by receptor-mediated endocytosis, escapes from endosomal vesicles to the cytosol, and then replicates in the nucleus. We examined the role of the microtubule (MT)-mediated cytoplasmic trafficking of viral particles toward the nucleus. Immunofluorescence and immunoelectron microscopy showed that capsids were transported through the cytoplasm into the nucleus after cytoplasmic microinjection but that in the presence of MT-depolymerizing agents, viral capsids were unable to reach the nucleus. The nuclear accumulation of capsids was also reduced by microinjection of an anti-dynein antibody. Moreover, electron microscopy and light microscopy experiments demonstrated that viral capsids associate with tubulin and dynein *in vitro*. Coprecipitation studies indicated that viral capsids interact with dynein. When the cytoplasmic transport process was studied in living cells by microinjecting fluorescently labeled capsids into the cytoplasm of cells containing fluorescent tubulin, capsids were found in close contact with MTs. These results suggest that intact MTs and the motor protein dynein are required for the cytoplasmic transport of CPV capsids and contribute to the accumulation of the capsid in the nucleus.

To begin a successful infection, viruses have developed a strategy that involves adsorption to cell surface receptors, penetration into the cytosol, uncoating of the viral genome, and targeting of the genome and accessory proteins to the correct cell area for nucleic acid replication. Most DNA viruses replicate in the nucleus, which provides the cellular factors required for the amplification and transcription of the viral genomes and for posttranscriptional processing of the viral mRNA. This suggests that after crossing the plasma membrane or endocytic membrane, released viruses or their components must also traverse the cytoplasm to enter the nucleus.

The cytoplasm imposes a diffusion barrier caused by high viscosity and steric obstacles. Cytoplasmic solutes and macromolecules, along with the lattice-like mesh of microtubules (MTs), actin, and intermediate filament networks, restrict the free diffusion of macromolecular complexes larger than 500 kDa (25, 44), indicating that virus-sized particles are unlikely to move efficiently through the cytosol by diffusion alone. It is likely that viruses would need to be actively transported during their cytoplasmic trafficking. MTs are polarized structures with a fast-growing plus end extending toward the cell periphery and a slow-growing minus end located at the centrosome or MT organizing center (MTOC), which is typically found in a perinuclear position (27). Directed transport of cellular components is linked to large complexes that form molecular motors. Cytoplasmic dynein and kinesin are known to mediate organelle movement in opposite directions along MTs. Cytoplasmic dynein, a minus-end-directed, MT-based motor, is a multisubunit protein complex of 1,270 kDa consisting of two

heavy chains (530 kDa), two or three intermediate chains (74 kDa), and a variable number of small subunits (19, 20). The ATPase and MT motor domains are located within the dynein heavy chains, whereas the specific cargo-binding activity involves the intermediate chains and several classes of light chains (7, 51). In many cases the MT-dependent transport of material is facilitated by the dynein activator protein dynactin, which mediates dynein binding to MTs (2, 18). Dynein, in conjunction with dynactin, facilitates membrane transport from the early endosomes to late endosomes and lysosomes (4, 17, 33, 50) and from the endoplasmic reticulum to the Golgi apparatus (40).

Ubiquitous as it is, the detailed process by which viruses transport their genome and associated proteins through the cytoplasm is still relatively poorly characterized. The involvement of MTs in cytoplasmic traffic has been reported for a number of viruses, and dynein-mediated transport has been described for adenovirus (22, 47, 48), human foamy virus (42), herpes simplex virus type 1 (HSV-1) (14, 45, 59), and African swine fever virus (ASFV) (3). In the case of HSV-1, the viral nucleocapsid protein ($\text{U}_{\text{L}34}$) interacts with a cytoplasmic dynein intermediate chain (59), while for ASFV, the viral protein p54 interacts with a cytoplasmic dynein light chain (3). In addition, vaccinia virus exploits MTs to enhance its exit from infected cells. Vaccinia virus particles, using MT plus-end-directed kinesin as a motor, are transported along MTs from the perinuclear site of assembly to the site of exit at the plasma membrane (38, 41).

The icosahedral, nonenveloped parvoviruses are among the smallest of the animal DNA viruses. The atomic structure of the canine parvovirus (CPV) capsid shows that the mature particle has a diameter of about 26 nm. The virion contains three capsid proteins (VP1, VP2, and VP3) with molecular sizes of 83, 67, and 65 kDa, respectively (1, 49, 58).

* Corresponding author. Mailing address: Department of Biological and Environmental Science, P.O. Box 35, University of Jyväskylä, Survantie 9, FIN-40500 Jyväskylä, Finland. Phone: (358) 14 2604209. Fax: (358) 14 2602271. E-mail: mviihinen@jyu.fi.

CPV uses the transferrin receptor as its cell surface receptor (34), and the infectious pathway involves clathrin-mediated, MT-dependent endocytosis followed by accumulation of viral capsids within perinuclear vesicles (35, 46, 52). After cell entry, capsids remain within endocytic compartments for several hours (35, 46). Although the mechanism of capsid escape from endosomal vesicles is still unknown, once in the cytosol, capsids move toward the nuclear membrane and enter the nucleus in a process which can be blocked by intracytoplasmic injection of antiviral antibodies up to several hours after virus inoculation (54, 55). MTs are required for nuclear localization of viral capsids, as evidenced by the fact that this process could be blocked by depolymerization of MTs in the presence of nocodazole. However, removal of nocodazole led to repolymerization of MTs and to nuclear transport of capsids (55).

The nuclear import of capsids appears to require modifications of viral capsids exposing potential nuclear localization sequences (NLS) within the VP1 N-terminal unique region (54). The N-terminal sequence (PAKRARRGYK) between residues 4 and 13 functions in nuclear transport when conjugated to bovine serum albumin (BSA) (53), and some specific changes in that VP1 N-terminal basic sequence reduced the relative infectivity of the capsids (54). Although the VP1 N terminus is inaccessible in capsids of CPV and minute virus of mice (MVM), that sequence is exposed *in vitro* without capsid disassembly (12, 54, 61). Both VP1 and VP2 are transported into the nucleus, and in MVM there are two NLS mapped near the VP1-specific N terminus, while transport of VP2 appears to involve an internal basic sequence (KGKLTMRRAKLR) (23, 24).

Here we examine further the translocation process of CPV capsids toward the nucleus. To test whether CPV capsids use an MT-associated mechanism for their transport, we first injected antibodies against dynein into the cell cytoplasm and subsequently injected cells with CPV; then we monitored capsid transport and viral infection. The anti-dynein antibody reduced nuclear transport relative to that in untreated cells. Furthermore, *in vitro* reconstitution and immunoprecipitation experiments suggested interactions between viral capsids and dynein. Immuno-electron microscopic (immuno-EM) studies showed that viral capsids entered the nuclei of cells after microinjection of capsids. These studies suggest that the cytoplasmic trafficking of the CPV capsids toward the nucleus is an MT-dependent process using cellular dynein and that viral capsids can enter the nucleus without extensive capsid disassembly.

MATERIALS AND METHODS

Cells and viruses. Norden Laboratory feline kidney (NLFK) cells were grown in Dulbecco's modified Eagle medium supplemented with 10% fetal calf serum (Gibco, Paisley, United Kingdom). CPV-d isolates were derived from an infectious plasmid clone by transfection of NLFK cells (34, 37). To prepare full capsids, viruses were propagated in NLFK cells; the capsids were purified by isopycnic centrifugation in a 45% CsCl gradient as described previously (46). Full capsids were used for preparation of Oregon green (OG)-labeled capsids according to the instructions for amine-reactive probes (Molecular Probes, Eugene, Oreg.). Immunoprecipitation experiments were carried out with viruses isolated from cell cultures infected for 5 to 7 days. Infected cells were frozen, thawed, and detached with a rubber policeman, and cell debris was removed by spinning at 2,000 rpm for 20 min. Viruses from the supernatant were concentrated by ultrafiltration (with a 500-kDa filter; Millipore Corp., Bedford, Mass.), and full CPV capsids were pelleted by ultracentrifugation at 173,000 $\times g$ for 2 h and resuspended in 1 ml of phosphate-buffered saline, pH 7.4 (PBS). The

suspension was sonicated at low power on ice and extracted with chloroform, and the aqueous phase was collected.

Antibodies and chemicals. A rabbit antibody to CPV capsid and a mouse monoclonal antibody (hybridoma culture medium; MAb 8) (36, 57) to CPV capsid were gifts from Colin Parrish (Cornell University, Ithaca, N.Y.). A mouse MAb to nonstructural protein 1 (NS1) was obtained from Caroline Astell (60) and conjugated to Texas red (TxR) (Molecular Probes). MTs were visualized by using a mouse MAb (Amersham, Little Chalfont, Buckinghamshire, United Kingdom) to tubulin. Anti-dynein antibodies (against the 74-kDa intermediate chain of cytoplasmic dynein) were obtained from Sigma (St. Louis, Mo.) or Chemicon (Temecula, Calif.). An anti-kinesin MAb was obtained from Chemicon. In the double-labeling studies, Alexa-546- or Alexa-488-conjugated anti-mouse antibodies and Alexa-488- or Alexa-546-conjugated anti-rabbit antibodies from Molecular Probes were used. Nanogold-conjugated polyclonal rabbit anti-mouse immunoglobulin G (IgG) was purchased from Nanoprobes (Yaphank, N.Y.). Epon LX-112 was obtained from Ladd Research industries (Williston, Vt.), and alkaline phosphatase-conjugated swine anti-rabbit immunoglobulins and aminoethylcarbazole substrate were from Dako (Glostrup, Denmark).

Nocodazole (Sigma) and vinblastine (Lilly France S.A., Fegersheim, France) were used for the depolymerization of MTs. Cycloheximide was obtained from Sigma, and OG-labeled bovine tubulin and taxol (paclitaxel) were obtained from Molecular Probes. Nanogold and HQ-silver enhancement reagents were obtained from Nanoprobes.

Microinjection antibody and drug treatments. Microinjection into NLFK cells was carried out using a semiautomatic system comprising Transector 5246 and Micromanipulator 5171 (Eppendorf, Hamburg, Germany) on an inverted microscope. Cells were grown to 80% confluence on microgrid coverslips (grid size, 175 nm; Eppendorf) and then injected into cytoplasm with 0.1 to 0.5 μl of antibody or viral capsids at 2.5 to 5 mg/ml. Anti-dynein and anti-kinesin antibodies, control mouse IgG, and viral capsids were concentrated and dialyzed against microinjection buffer (10 mM Tris-HCl-120 mM KCl [pH 7.4]).

Full capsids were injected together with the anti-dynein or anti-kinesin antibodies or with control mouse IgG. After 6 h of incubation, cells were fixed with 4% paraformaldehyde (PFA) (for 20 min at room temperature [RT]) and then incubated with PBS containing 0.1% Triton X-100, 1% BSA, and 0.01% sodium azide for 20 min at RT prior to immunolabeling of capsids and injected antibody.

To test for changes in the organization of the MT network for cytoplasmic trafficking of capsids, cells were incubated in a medium containing 60 μM nocodazole, 20 μM vinblastine, or 2 μM taxol for 30 min prior to capsid injection. The drug was then maintained until fixation in methanol. Cells were stained with an anti-tubulin antibody to confirm the effect of the drug on the MT structure. Laser scanning microscopy (LSM) was conducted on a Zeiss LSM 510 inverted microscope. Cycloheximide (0.2 mM) was added to the medium to prevent synthesis of new viral proteins and progeny virus during incubations of more than 6 h involving analysis of the localization of incoming virus particles in inoculated cells or in microinjected cells.

CPV infection was detected by staining for the viral NS1 protein with a TxR-conjugated anti-NS1 MAb after methanol fixation (for 6 min at -20°C). The proportion of NS1-expressing cells in normally inoculated cells or in cells injected with capsids was determined at different time points. In addition, the effects of MT-depolymerizing drugs on the number of NS1-expressing cells were examined in normally inoculated or microinjected cells.

Preamplification labeling for electron microscopy. NLFK cells on 35-mm-diameter plastic culture dishes were grown to ~80% confluence. In injection experiments, cells were incubated for 2 or 6 h at 37°C after injection of full capsids (2.5 mg/ml). For infection assays, cells were incubated with 0.05 μg of capsids/ml for 10 or 12 h prior to fixation. Cells were washed twice with PBS and then fixed for 2 h at RT in periodate-lysine-PFA fixative (9). Fixed cells were prepared for preamplification EM as described previously (39, 43). Cells were treated with 0.01% saponin and 0.1% BSA in 0.1 M phosphate buffer, pH 7.4 (buffer A), before addition of the anti-capsid MAb diluted in buffer A. Half of the samples were treated with 0.05% Triton X-100 in buffer A to ensure that the nuclear membrane was permeabilized. After 1 h of incubation at RT and washes with buffer A, nanogold-conjugated polyclonal rabbit anti-mouse IgG was applied for 1 h, followed by washes with buffer A and 0.1 M phosphate buffer (pH 7.4). Cells were postfixed with 1% glutaraldehyde in phosphate buffer for 10 min at RT, quenched with 50 mM NH₄Cl in phosphate buffer, and then washed with phosphate buffer and water. Cells were treated in the dark with HQ-silver for 2 min, followed by washes with water and gold toning (exposure to 2% sodium acetate [three times, for 5 min each time], 0.05% gold chloride [for 10 min on ice], and 0.3% sodium thiosulfate [twice, for 10 min each time, on ice]). After washes with water, the cell cultures were reduced in 1% osmium tetroxide in 0.1 M phosphate buffer for 1 h at 4°C, dehydrated with a graded series of ethanol, and then stained

with 2% uranyl acetate. Plastic capsules filled with Epon LX-112 were placed upside down on top of the cells. After polymerization, the capsules were warmed up to 100°C and removed carefully, and sections parallel to the bottom were cut with an ultramicrotome (Ultracut 8008; Reichert-Jung) set to 50 nm, picked up on a copper grid, stained with 2% uranyl acetate and lead citrate, and viewed with an EM.

MT binding assays. In vitro microscopic assays were set up to observe the interaction between the CPV, MT, and dynein. TxR-labeled α -tubulin was polymerized and stabilized with taxol as recommended by the manufacturer. For the LSM microscopy, OG-labeled capsids were mixed with polymerized MTs and the postnuclear supernatant (PNS) in a 1:1:1 ratio (giving a final concentration of 1.5 μ g/ml each) in FDB buffer [35 mM piperazine-*N,N*-9-bis(2-ethanesulfonic acid) (PIPES), 1 mM EGTA, 0.5 mM EDTA, 1 to 4 mM GTP] containing 10 μ M taxol (20) and incubated for 30 min at room temperature. The mixture was transferred to a glass chamber coated with DEAE-dextran (2 mg/ml) (31) and viewed without fixation.

For EM, concentrated capsids (containing dynein according to immuno-EM and immunoprecipitation studies) were mixed with MTs in a 1:1 ratio. The mixture was incubated on the grids for 1 h and stained with uranyl oxalate, followed by a methyl cellulose-uranyl acetate embedding step (16). In parallel, samples were fixed with 4% PFA and immunolabeled. CPV was labeled with an anti-capsid antibody followed by gold-conjugated protein A (5-nm-diameter beads), after which free antibodies were blocked with protein A. Dynein was labeled with an anti-dynein MAb, followed by gold-conjugated protein A (10-nm-diameter beads). Then samples were negatively stained and embedded with methyl cellulose-uranyl acetate.

Finally, the distribution of capsids and their relationship to the MT network were studied in the cytoplasm of living cells. Cells were first injected with rhodamine-labeled tubulin diluted in PBS (2.5 mg/ml). After incubation at 37°C for 3 to 4 h, the same cells were then reinjected with OG-labeled viral capsids (2.5 mg/ml) and incubated for 1 to 2 h at 37°C. The cells were then monitored by LSM without fixation.

Coimmunoprecipitation and Western blotting. For coprecipitation experiments, concentrated viral capsids were immunoprecipitated with anti-dynein antibodies. Lysates prepared from noninfected cells were used as a control. Before precipitation, viruses and cell lysates were mixed with protein A beads (Prosep-A High Capacity; Bioprocessing Ltd., Durham, England) for 1 h at 4°C, followed by centrifugation at 12,000 $\times g$ for 20 s. Supernatants were used for immunoprecipitation. Precleared viruses were immunoprecipitated with a mixture of two anti-dynein MAbs or with a control MAb against trout Ig (2 to 5 μ g of antibody/1 mg of protein). The mixture was incubated overnight at 4°C; then immune complexes were collected by absorption onto protein A beads (for 1.5 h at 4°C). The precipitates were washed (four times) with PBS containing 0.1% Tween 20 (PBS-Tween). For Western blotting, precipitated proteins were separated on a sodium dodecyl sulfate-polyacrylamide gel electrophoresis running gel (7.5% acrylamide) (21). The proteins were transferred to nitrocellulose membranes and incubated overnight with 10 mM Tris-buffered saline, pH 7.4 (TBS), containing 3% BSA; then capsids were detected with a rabbit antibody against denatured CPV capsids. After a wash with TBS and 0.2% Tween, the membranes were incubated first with horseradish peroxidase-conjugated goat anti-rabbit immunoglobulins and then with an aminoethylcarbazole substrate (Dako).

RESULTS

It has been shown previously that capsids injected into the cytoplasm of cells were transported through the cytoplasm toward and into the nucleus in a process that could be blocked by nocodazole treatment (55). Here we further examined the role of the cytoskeleton in cytoplasmic trafficking of viral capsids and the connection between capsids, dynein, and MTs and the nuclear import of the capsids.

Cytoskeleton-dependent, nucleus-directed transport of cytosolic virus. To determine the efficiency of the nuclear transport of cytoplasmic capsids, viral capsids were injected into cells in the presence or absence of drugs affecting MTs and in the presence of 0.2 mM cycloheximide. In nontreated cells after 10 h of incubation, approximately 42% of injected cells showed strong nuclear labeling, suggesting that many capsids had ac-

cumulated in the nucleus (Fig. 1). In the remaining injected cells, numerous small fluorescent spots that represented either individual capsids or capsid clusters were distributed throughout the cell. Disruption of the MT network by nocodazole or vinblastine treatments reduced the amount of nuclear import of viruses, so that only 8 or 1% of cells showed nuclear accumulation of viral capsids. Cells treated with taxol, an MT stabilizer, also had reduced nuclear import levels, showing 22% fluorescent nuclei (Fig. 1).

To demonstrate whether drug-treated or nontreated cells (without cycloheximide) injected with capsids became infected, cells were also immunolabeled for newly produced viral NS1 protein. Interestingly, 25% of cells treated with nocodazole and 15% of cells treated with vinblastine showed detectable NS1 protein at 12 h postinjection (Fig. 2A), indicating that the treatments did not inhibit the nuclear import of capsids enough to prevent infection. Furthermore, 35% of injected cells in the presence of taxol and 53% of injected cells in the absence of drugs showed detectable levels of NS1 expression (Fig. 2A).

In addition, to confirm whether the above results with microinjected capsids were consistent with productive infection, we analyzed the NS1 production of CPV-inoculated cells at 10 h after normal viral infection. Only 1.5% of nocodazole-treated cells and 0% of vinblastine-treated cells expressed NS1, whereas 43% of untreated and 16% of taxol-treated cells showed the presence of NS1 (Fig. 2B). The lower expression of NS1 in inoculated, drug-treated cells may be due to the combination of blockage of the endocytic pathway of the virus and effects on cytoplasmic transport.

The kinetics of NS1 expression was examined by injecting capsids into the cytoplasm or by inoculating the cells with the virus, and then determining the proportions of NS1-expressing cells at various time points. An increase in the proportion of NS1-expressing cells was observed after 8 h in both injected cells and inoculated cells, and the maximum percentage of infected cells was reached after 12 h (Fig. 2C).

Transport of capsids to the nucleus in the presence of antibodies against MT motor proteins. We tested whether antibodies against motor proteins would affect the nuclear transport of capsids. We coinjected target cells with capsids and a MAb to the 74-kDa intermediate chain of the dynein motor complex. The presence of the anti-dynein antibody causes the disruption of the minus end-directed movement of dynein, as has been observed for adenovirus capsids (22). The cytoplasmic anti-dynein MAb decreased the amount of nuclear capsids, whereas in parallel sets of cells injected with capsids and either an anti-kinesin MAb or control mouse IgG, no effect on nuclear transport was seen (Fig. 3). Seven to 13% of cells coinjected with an anti-dynein MAb and capsids showed trace amounts of capsids accumulating in the nucleus, suggesting that nuclear transport was mostly blocked by the antibody. However, some trafficking might still have occurred, or that capsids reached the nucleus by diffusion or as a result of the microinjection process. When the capsids were coinjected with an anti-kinesin MAb or control mouse IgG, clear nuclear localization of capsids was detected in 40 to 50% of the injected cells.

EM analysis of nuclear transport of capsids. To monitor intracellular transport, capsids were labeled with a MAb

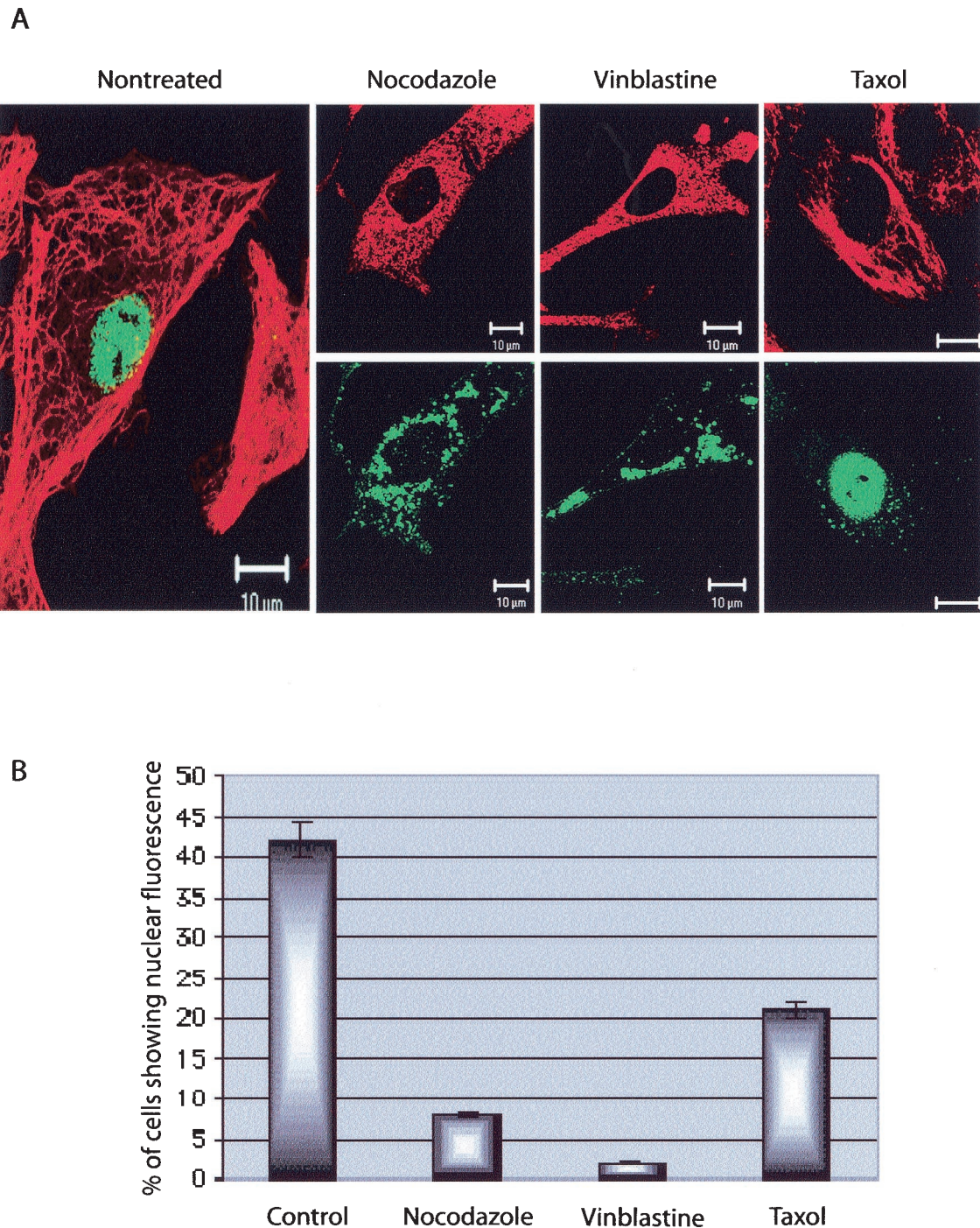


FIG. 1. Intracellular localization of CPV capsids 10 h after injection into cytoplasm of cells in the presence or absence of drugs affecting the MT cytoskeleton. (A) Localization of capsids after cytoplasmic injection. Bars, 10 μ m. (B) Percentages of cells injected with capsids showing substantial nuclear localization ($n, \approx 300$). All experiments were performed in the presence of 0.2 mM cycloheximide, and 2.5 mg of virus/ml was used for injections. The injected capsids were detected with a specific rabbit anti-capsid IgG followed by Alexa-488-labeled anti-rabbit IgG (green), and MTs were detected with an antibody against tubulin followed by an Alexa-546-conjugated anti-mouse antibody (red).

against intact viral capsids, and nanogold-immunolabeling EM with a silver enhancement technique was used. By use of this method, intracellular capsids were visualized as small, intensely labeled, grainy spots (Fig. 4). Purified full CPV capsids were injected into the cytosol of cells, and capsid antigen was

detected inside the nucleus at 2 h after injection (Fig. 4A). Capsids recognized by MAb 8, which binds intact capsids (56), were also seen inside the cytoplasm. In some of the images, capsids seemed to be adjacent to the nuclear membrane (Fig. 4B). In cells inoculated with capsids, the incoming CPV capsids

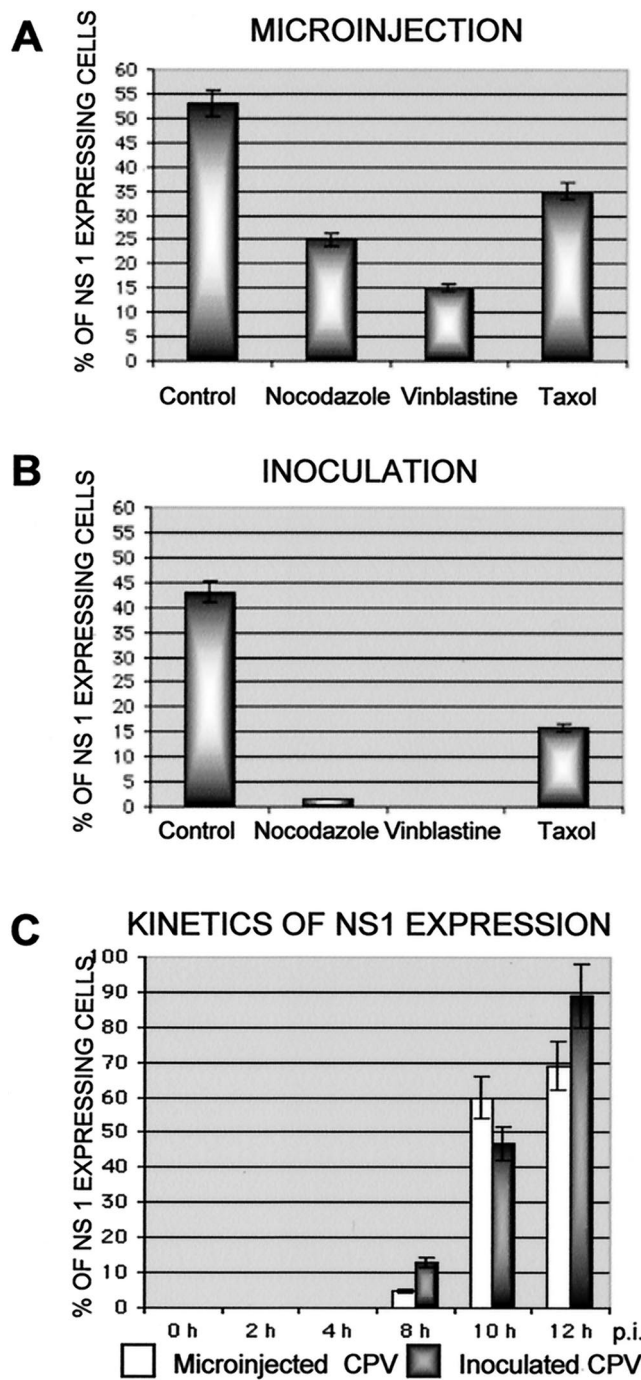


FIG. 2. Intracellular expression of the viral NS1 protein in infected cells or in cells microinjected with capsids. Expression of NS1 was detected with a TxR-labeled MAb against NS1 protein. (A and B) Percentage of cells showing substantial NS1 expression 10 h after viral inoculation ($n, \approx 300$) (B) or cytoplasmic microinjection (A) with CPV capsids ($n, \approx 300$) in the presence or absence of MT-affecting drugs. (C) Kinetics of NS1 expression in cells inoculated with virus or microinjected with capsids. The percentage of cells showing detectable amounts of NS1 protein in the nucleus or cytoplasm was determined at various times between 0 and 12 h ($n, \approx 300$).

were found in vesicular structures located near the nuclear membrane after 10 h of incubation of cells (data not shown), and some cytoplasmic capsids appeared associated with the nuclear membrane (Fig. 4C and D). Very few capsids were observed in the nuclei of infected cells (Fig. 4D). Experiments were performed in the presence of 0.2 mM cycloheximide to block the synthesis of new viral proteins. The slight degeneration of the fine structure of cells was due to the Triton X treatment used to permeabilize the nuclear membrane to allow antigen labeling inside the nucleus.

MT binding assays. To analyze virus-MT interaction in more detail, we investigated whether viral capsids would bind MTs in vitro. In confocal microscopy, OG-labeled capsids were found in the proximity of taxol-stabilized TxR-labeled MTs, and capsids could be seen to follow the MT tracks; they were clearly aligned on MTs in the presence of PNS. However, when the same experiment was repeated in the absence of PNS, capsids showed little interaction with MTs (Fig. 5).

In in vitro EM analysis of stabilized MTs and viral capsids, negatively stained capsid-like structures localized in contact with MTs (Fig. 6A). Immuno-EM with the anti-capsid antibody followed by protein A-coupled gold particles (diameter, 5 nm) showed capsid-like structures bound to MTs with colloidal gold particles in close proximity (Fig. 6B). To examine whether cytoplasmic dynein associated with the capsids, a double-immunolabeling in vitro EM assay was performed. Figure 6B shows double labeling of the capsid-like structures with an anti-capsid antibody (5-nm-diameter gold particles) and an anti-dynein antibody (10-nm-diameter gold particles). In contrast, capsids purified by CsCl centrifugation showed no labeling for dynein (data not shown), suggesting that dynein might not remain bound to the capsid upon purification. These purified capsids showed little binding to MTs (data not shown).

To examine the association of capsids with MTs within the cytosol of living cells, we microinjected fluorescently labeled capsids into cells containing injected, fluorescently labeled tubulin. Images collected from cells 4 h after injection with rhodamine-tubulin indicated that labeled tubulin was integrated into the entire MT network (data not shown). When the cells were reinjected with OG-labeled capsids, the fluorescent capsids were localized in close proximity to MTs throughout the cytoplasm (Fig. 7).

Coimmunoprecipitation. Double-labeling EM demonstrated an association between CPV capsids and dynein. To further investigate the interaction of capsids with dynein, antibodies against the cytoplasmic dynein intermediate chain were used to immunoprecipitate concentrated viral capsids. When precipitates were studied by immunoblotting with an antibody against denatured viral capsids, a band the size of VP2 (67 kDa) was observed (Fig. 8). The anti-dynein antibody did not coprecipitate capsids purified by CsCl centrifugation (data not shown), indicating that dynein-capsid complexes disintegrate during capsid purification.

DISCUSSION

Passive cytosolic trafficking of virus-sized particles is generally restricted by the properties of the cytoplasm, and structures with diameters greater than 50 nm are unlikely to move within the cells by diffusion alone, suggesting that their efficient

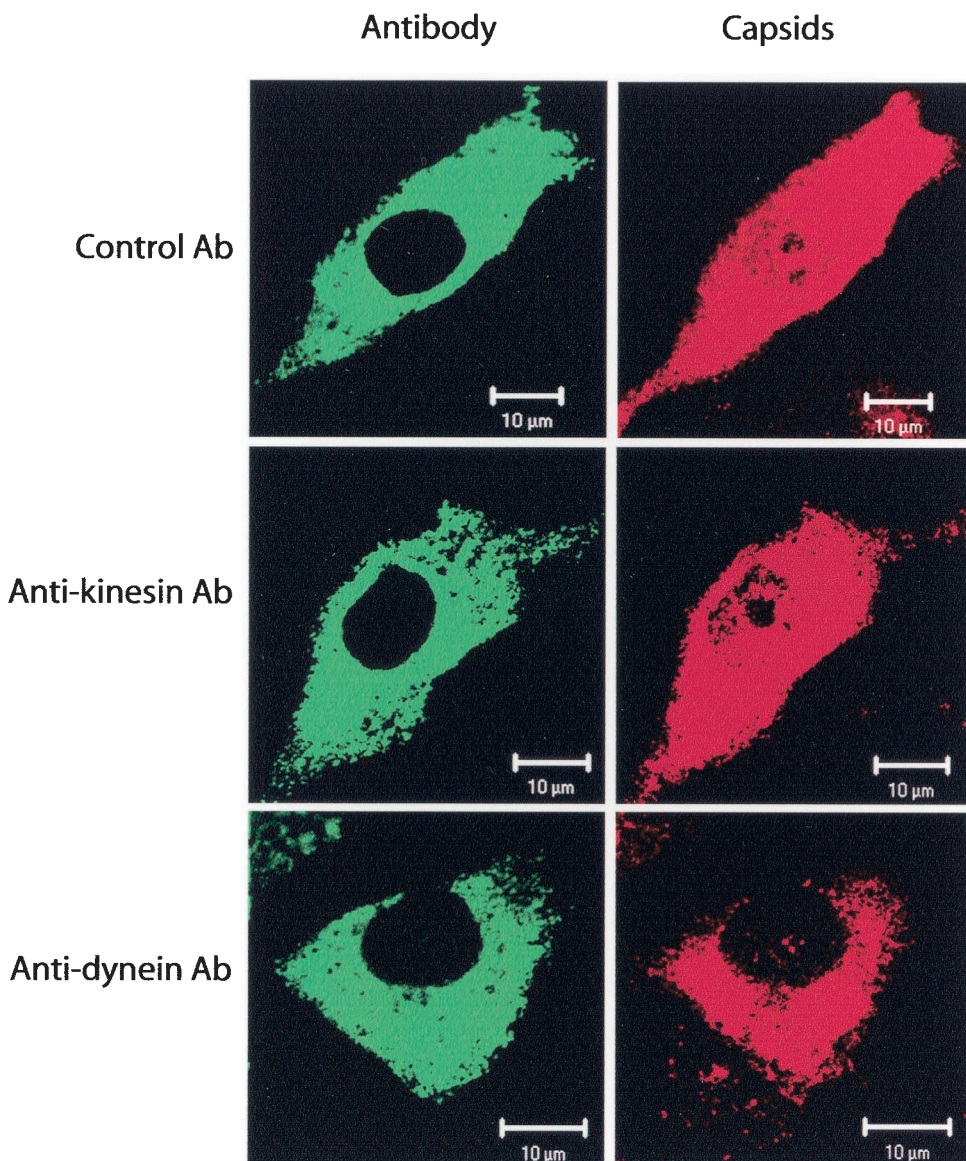


FIG. 3. Intracellular localization of CPV capsids microinjected into cytoplasm along with antibodies against the motor protein dynein or kinesin. The cells were incubated for 6 h after injection, after which they were fixed and stained for capsids with rabbit polyclonal anti-capsid IgG followed by Alexa-546-conjugated goat anti-rabbit IgG (red). The presence of the injected anti-dynein MAb, the anti-kinesin MAb, and control mouse IgG was detected using Alexa-488-conjugated goat anti-mouse IgG (green).

intracellular transport requires interactions with the host transport system (25, 26, 44). Earlier results showed that the 26-nm-diameter CPV particles require intact MTs during the infection. Although nocodazole blocked the viral infection (46, 52), it was quite difficult to determine the steps in viral entry affected and whether the block was due to effects on endocytosis or to direct interaction between viral components and the MTs. Direct microinjection of capsids resulted in a relatively slow but efficient nuclear uptake of capsids, which was blocked by nocodazole treatment, suggesting that MTs controlled the transport of capsids across the cytoplasm to the nucleus (55). These experiments did not define the mechanism responsible for the cytoplasmic transport of capsids.

To define the role of MTs in nuclear localization, we tested

three drugs that affect the MT cytoskeleton for their effects on the nuclear transport of cytoplasmically injected capsids. In the presence of nocodazole, which depolymerizes MTs, and vinblastine, which causes MT paracrystal formation, injected viral capsids were found dispersed in the cytoplasm. They did not reach the perinuclear region in significant amounts, suggesting that an essential MT-dependent step preceded the nuclear import of capsids (Fig. 1A). There was also a slightly decreased level of nuclear import of capsids in the presence of taxol, which stabilizes MTs (Fig. 1B). These data imply that MTs can serve as tracks to mediate the transport of virus toward the nucleus and that the polymerization and depolymerization events at MT ends might also affect nucleus-oriented viral movements.

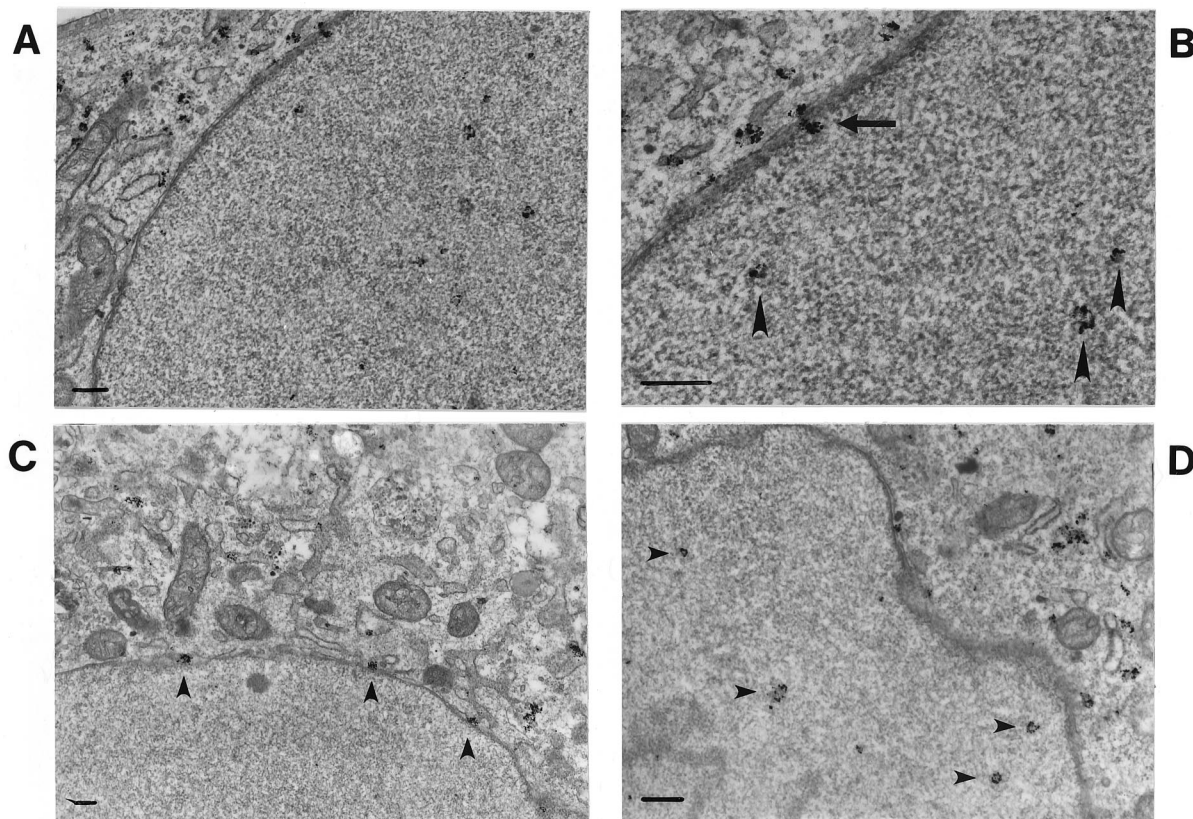


FIG. 4. Intracellular distribution of CPV capsids in cytoplasmically microinjected or in normally infected cells. Capsids were detected by use of a preembedding immunolabeling technique where labeling with MAb 8, an antibody generated against intact capsids, was followed by silver-enhanced nanogold (1.4-nm-diameter particles) and gold toning treatments. (A) Cells injected with capsids (2.5 mg/ml) and then incubated for 2 h. (B) Close-up shows intranuclear capsids (arrowheads) and a nuclear membrane with a viral capsid attached to it (arrow). (C) In infected cells fixed at 10 h postinfection, viral capsids were detected on the nuclear membrane (arrowheads). (D) Infected cells fixed at 12 h postinfection showed cytoplasmic localization of capsids in addition to trace amount of nuclear capsids (arrowheads). All experiments were performed in the presence of cycloheximide (0.2 mM). Bars, 200 nm.

Successful infection of cells was monitored by immunostaining for the viral NS1 protein. NS1 protein serves both as an initiator protein for viral DNA replication and as a transcriptional activator of the viral promoters (11, 13, 32). Thus, NS1 is found in infected cells before the synthesis of structural proteins (10, 30). NS1 protein is an efficient marker for the import of capsids to the nucleus, leading to viral gene expression and productive infection.

For cells injected with capsids, expression of NS1 protein was significantly decreased, although not completely absent, in the presence of MT-destroying drugs (Fig. 2A). The NS1 expression may be due to some of the injected capsids reaching the nucleus in an MT-independent fashion, perhaps as a direct result of the microinjection, or due to the large numbers of capsids injected. In cells inoculated with virus, NS1 expression was inhibited almost completely by nocodazole or vinblastine treatment (Fig. 2B), most likely due to the multilevel inhibition of transport caused by the MT disruption. Since intact MTs and functional motor proteins are essential for endosomal vesicular trafficking, endosomal transport and sorting, and maintenance of the location of late endosomes and recycling endosomes (5, 8, 17, 28, 29, 33), the disintegration of MTs might cause a disturbance in the endocytic entry of the virus

capsids. Our studies suggest that CPV escapes into the cytosol during the late steps of the endocytic pathway (Suikkanen et al., unpublished data). In addition, it has been shown that inoculation of cells with depleted MT-dependent transport causes entering capsids to be retained in vesicles dispersed to the peripheries of the cells (46). Our present results seem to suggest that capsids entering MT-deficient cells were not able to traffic through the endosomal pathway to the site of release but instead remained inside endosomal structures without being able to cause a productive infection. Taken together, these results suggest that in the absence of MT, fewer viral genomes were transported to the cell nucleus and the level of viral NS1 protein synthesis was significantly reduced.

The production of NS1 started 8 h after either injection or infection of cells (Fig. 2C). Even though cytoplasmically microinjected viruses were detected within the nucleus 2 h post-microinjection (Fig. 4A and B), they appear to require several hours to reach levels of NS1 expression detectable with a fluorescent microscope.

To accomplish the movement toward the nucleus, viral capsids are likely to benefit from the inherent polarity of MTs by using MT-associated motors. Since minus ends of MTs are anchored at the perinuclear MTOC, it seems likely that dynein

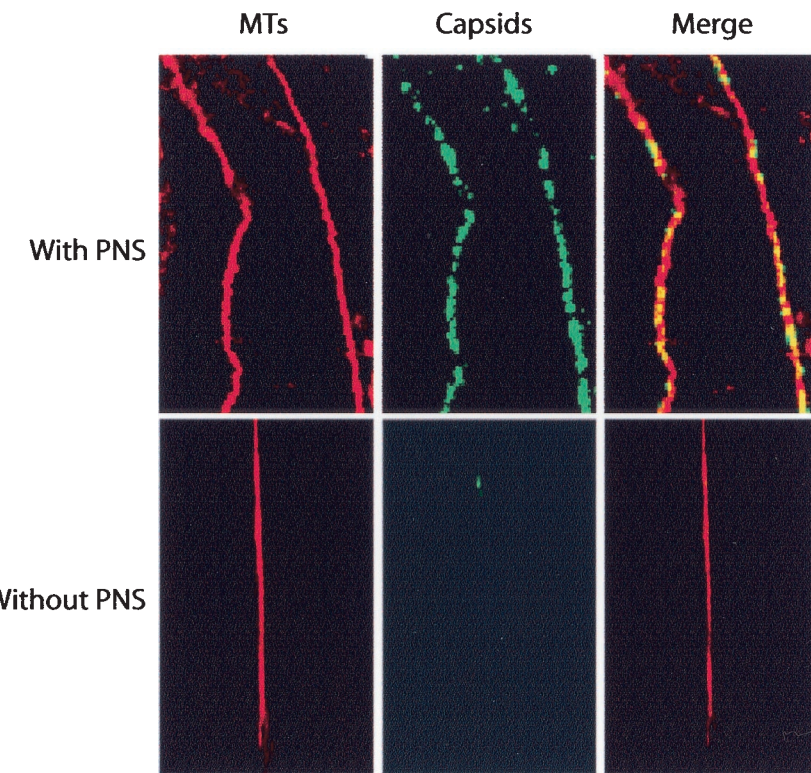


FIG. 5. In vitro binding of CPV capsids to MTs. Shown is the interaction of OG-labeled purified viral capsids with TxR-labeled MTs stabilized with taxol in the presence or in the absence of PNS.

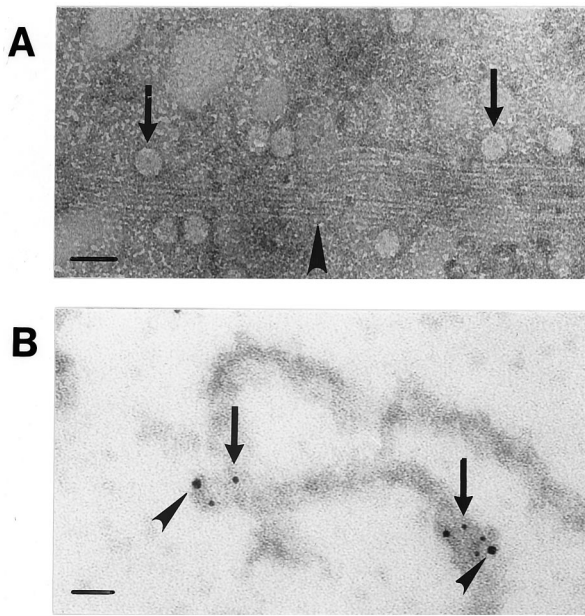


FIG. 6. Interaction between the CPV viral capsids, MTs, and dynein in vitro. (A) EM image of negatively stained preparation containing taxol-stabilized MTs (arrowhead) and purified capsids (arrows). (B) Immunogold-labeled viral capsids (5-nm-diameter gold particles) containing the intermediate chain of dynein (10-nm-diameter gold particles) (arrowheads) bound to MT. Bars, 50 nm.

is used to transport incoming viral capsids toward the nucleus. Coinjection of antibodies against dynein along with capsids showed that the transport of capsids into the nucleus was markedly decreased in the presence of the antibody, suggesting that the intermediate chain of dynein is involved in capsid transport toward the nucleus. Antibodies against the plus-end-directed motor kinesin did not affect CPV trafficking to the

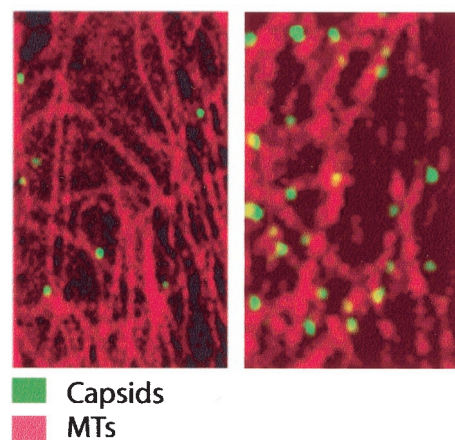


FIG. 7. Localization of CPV capsids in living cells. Cells were microinjected with rhodamine-labeled tubulin and incubated for 4 h at 37°C to label MTs; then they were injected with OG-labeled capsids and incubated for 2 h at 37°C. Cells were visualized with LSM without fixation.

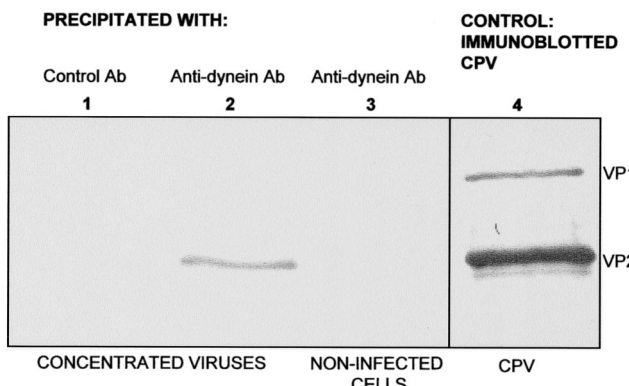


FIG. 8. Coimmunoprecipitation of CPV capsids with an anti-dynein antibody. Viruses concentrated from cells infected with CPV (lane 2) and a cell extract from noninfected cells (lane 3) were immunoprecipitated with MAbs against dynein. A control precipitation (lane 1) was performed with a MAb against trout Ig, and all samples were immunoblotted with an antibody against viral capsid protein. The migration positions of CPV capsid proteins VP1 (M_r , 83,000) and VP2 (M_r , 67,000) are shown in lane 4.

nucleus (Fig. 3). Whether the binding of dynein to CPV capsids involved other cellular components remains unclear.

NLS-mediated translocation through the nuclear pore complex (NPC) of the nuclear envelope occurs by sequential steps that involve a series of interactions between cargo, soluble transport factors, and nuclear pore proteins of the central transport channel (6). The mechanism of nuclear import restricts the passive diffusion of molecules of approximately 25 Å (2.5 nm) but allows NLS-containing substrates as large as 300 Å or more to rapidly enter the nucleus (15). Parvoviruses are potentially small enough to pass through the nuclear pore without capsid disassembly or deformation. It has not yet been established whether parvoviruses are able to pass through the NPC intact, without capsid disassembly, during the early steps of infection. The VP1 N-terminal end, containing several potential NLS, appears to play a role in the nuclear import process. After injection into the cytoplasm, the VP1 N-terminal sequence of the capsid was exposed in a manner which was correlated with the nuclear transport of the capsids (54). The EM studies presented here demonstrate further that viral capsids injected into cytoplasm and entering the nucleus are recognized by a MAb recognizing only intact capsids (56), indicating that nuclear entry occurs without extensive uncoating (Fig. 4A and B). During normal infection, some cells showed trace amounts of intranuclear labeling, suggesting that only a few virions are imported to the nucleus, whereas most capsids remain in the endosomal vesicles or in the cytoplasm (Fig. 4C and D).

Both in vitro and in vivo assays were used to analyze the binding of capsids to MTs. Capsids actively bound to MTs in vitro became aligned along MT tracks (Fig. 5). In vitro binding assays using EM confirmed the MT-binding activity of capsids and showed that capsids could be simultaneously bound to both dynein and MTs (Fig. 6A and B). The association of capsids with dynein was further verified by coprecipitation of capsids isolated from infected cells by using antibodies to dynein (Fig. 8). The interaction of capsids with MTs in vitro is

consistent with the in vivo observation that cytoplasmic viruses were associated MTs in living cells (Fig. 7). Taken together, these data imply that capsids were bound to MTs both in vitro and in vivo, in addition to the involvement of dynein in this interaction.

Taken together, the data described here confirm that cytoplasmic trafficking of capsids requires intact MTs and demonstrate the ability of dynein MT motor proteins to bind capsids, suggesting that dynein may play an important role during the binding and transporting of capsids along MTs to the site of their nuclear import. Our results suggest that parvoviral capsids released to the cytoplasm are likely to traffic along MTs toward the nucleus during productive infection. It will now be important to determine how the interactions among capsids, dynein, and MTs are regulated in order to explain the molecular mechanism leading to infection.

ACKNOWLEDGMENTS

We are especially grateful to Colin Parrish for fruitful discussions, helpful comments on the manuscript, and antibodies. We thank Gareth Griffiths for help with EM and Pirjo Kauppinen, Jonna Hirsimäki, Einari Niskanen, Paavo Niutanen, and Raimo Pesonen for excellent technical assistance.

This work was supported by grants from the Academy of Finland (contract 10210), the National Technology Agency (TEKES; contract 70026/00), and the Finnish Cultural Foundation.

REFERENCES

- Agbandje, M., R. McKenna, M. G. Rossmann, M. L. Strassheim, and C. R. Parrish. 1993. Structure determination of feline panleukopenia virus empty particles. *Proteins* **16**:155-171.
- Allan, V. 1996. Motor proteins: a dynamic duo. *Curr. Biol.* **6**:630-633.
- Alonso, C., J. Miskin, B. Hernaez, P. Fernandez-Zapatero, L. Soto, C. Canto, I. Rodriguez-Crespo, L. Dixon, and J. M. Escrivano. 2001. African swine fever virus protein p54 interacts with the microtubular motor complex through direct binding to light-chain dynein. *J. Virol.* **75**:9819-9827.
- Aniento, F., N. Emans, G. Griffiths, and J. Gruenberg. 1993. Cytoplasmic dynein-dependent vesicular transport from early to late endosomes. *J. Cell Biol.* **123**:1373-1387.
- Bananis, E., J. W. Murray, R. J. Stockert, P. Satir, and A. W. Wolkoff. 2000. Microtubule and motor-dependent endocytic vesicle sorting in vitro. *J. Cell Biol.* **151**:179-186.
- Bayliss, R., A. H. Corbett, and M. Stewart. 2000. The molecular mechanism of transport of macromolecules through nuclear pore complexes. *Traffic* **1**:448-456.
- Boylan, K., M. Serr, and T. Hays. 2000. A molecular genetic analysis of the interaction between the cytoplasmic dynein intermediate chain and the glued (dynactin) complex. *Mol. Biol. Cell* **11**:3791-3803.
- Brown, K. D., M. Friedkin, and E. Rozengurt. 1980. Colchicine inhibits epidermal growth factor degradation in 3T3 cells. *Proc. Natl. Acad. Sci. USA* **77**:480-484.
- Brown, W. J., and M. G. Farquhar. 1989. Immunoperoxidase methods for the localization of antigens in cultured cells and tissue sections by electron microscopy. *Methods Cell Biol.* **31**:553-569.
- Cotmore, S. F., and P. Tattersall. 1987. The autonomously replicating parvoviruses of vertebrates. *Adv. Virus Res.* **33**:91-169.
- Cotmore, S. F., J. Christensen, J. P. F. Nuesch, and P. Tattersall. 1995. The NS1 polypeptide of the murine parvovirus minute virus of mice binds to DNA sequences containing the motif [ACCA]₂₋₃. *J. Virol.* **69**:1652-1660.
- Cotmore, S. F., A. M. D'Abromo, Jr., C. M. Ticknor, and P. Tattersall. 1999. Controlled conformational transitions in the MVM virion expose the VP1 N-terminus and viral genome without particle disassembly. *Virology* **254**:169-181.
- Cotmore, S. F., and P. Tattersall. 1994. An asymmetric nucleotide in the parvoviral 3' hairpin directs segregation of a single active origin of DNA replication. *EMBO J.* **13**:4145-4152.
- Dohner, K., A. Wolfstein, U. Prank, C. Echeverri, D. Dujardin, R. Vallee, and B. Sodeik. 2002. Function of dynein and dynactin in herpes simplex virus capsid transport. *Mol. Biol. Cell* **13**:2795-2809.
- Feldherr, C. M., D. Akin, and R. J. Cohen. 2001. Regulation of functional nuclear pore size in fibroblasts. *J. Cell Sci.* **114**:4621-4627.
- Griffiths, G., A. McDowell, R. Back, and J. Dubochet. 1984. On the preparation of cryosections for immunocytochemistry. *J. Ultrastruct. Res.* **89**:65-78.

17. Gruenberg, J., G. Griffiths, and K. E. Howell. 1989. Characterization of the early endosome and putative endocytic carrier vesicles in vivo and with assay of vesicle fusion in vitro. *J. Cell Biol.* **108**:1301–1316.
18. Holleran, E. A., S. Karki, and E. L. Holzbaur. 1998. The role of the dynactin complex in intracellular motility. *Int. Rev. Cytol.* **182**:69–109.
19. Holzbaur, E. L., and R. B. Vallee. 1994. Dyneins: molecular structure and cellular function. *Annu. Rev. Cell Biol.* **10**:339–372.
20. King, S. J., and T. A. Schroer. 2000. Dynactin increases the processivity of the cytoplasmic dynein motor. *Nat. Cell Biol.* **2**:20–24.
21. Laemmli, U. K. 1970. Cleavage of structural proteins during the assembly of the head of bacteriophage T4. *Nature* **227**:680–685.
22. Leopold, P. L., G. Kreitzer, N. Miyazawa, S. Rempel, K. K. Pfister, B. E. Rodriguez, and R. G. Crystal. 2000. Dynein- and microtubule-mediated translocation of adenovirus serotype 5 occurs after endosomal lysis. *Hum. Gene Ther.* **11**:151–165.
23. Lombardo, E., J. C. Ramirez, M. Agbandje-McKenna, and J. M. Almendral. 2000. A beta-stranded motif drives capsid protein oligomers of the parvovirus minute virus of mice into the nucleus for viral assembly. *J. Virol.* **74**:3804–3814.
24. Lombardo, E., J. C. Ramirez, J. Garcia, and J. M. Almendral. 2002. Complementary roles of multiple nuclear targeting signals in the capsid proteins of the parvovirus minute virus of mice during assembly and onset of infection. *J. Virol.* **76**:7049–7059.
25. Luby-Phelps, K. 2000. Cytoarchitecture and physical properties of cytoplasm: volume, viscosity, diffusion, intracellular surface area. *Int. Rev. Cytol.* **192**:189–221.
26. Luby-Phelps, K. 1994. Physical properties of cytoplasm. *Curr. Opin. Cell Biol.* **6**:3–9.
27. Mandelkow, E., and E. M. Mandelkow. 1995. Microtubules and microtubule-associated proteins. *Curr. Opin. Cell Biol.* **7**:72–81.
28. Matteoni, R., and T. E. Kreis. 1987. Translocation and clustering of endosomes and lysosomes depends on microtubules. *Eur. J. Cell Biol.* **105**:1253–1265.
29. McGraw, T. E., K. W. Dunn, and F. R. Maxfield. 1993. Isolation of a temperature-sensitive variant Chinese hamster ovary cell line with a morphologically altered endocytic recycling compartment. *J. Cell. Physiol.* **155**:579–594.
30. Molitor, T. W., H. S. Joo, and M. S. Collett. 1985. Identification and characterization of a porcine parvovirus nonstructural polypeptide. *J. Virol.* **55**:554–559.
31. Murray, J. W., E. Bananis, and A. W. Wolkoff. 2000. Reconstitution of ATP-dependent movement of endocytic vesicles along microtubules in vitro: an oscillatory bidirectional process. *Mol. Biol. Cell* **11**:419–433.
32. Nuesch, J. P., S. F. Cotmore, and P. Tattersall. 1995. Sequence motifs in the replicator protein of parvovirus MVM essential for nicking and covalent attachment to the viral origin: identification of the linking tyrosine. *Virology* **209**:122–135.
33. Oda, H., R. J. Stockert, C. Collins, H. Wang, P. M. Novikoff, P. Satir, and A. W. Wolkoff. 1995. Interaction of the microtubule cytoskeleton with endocytic vesicles and cytoplasmic dynein in cultured rat hepatocytes. *J. Biol. Chem.* **270**:15242–15249.
34. Parker, J. S., W. J. Murphy, D. Wang, S. J. O'Brien, and C. R. Parrish. 2001. Canine and feline parvoviruses can use human or feline transferrin receptors to bind, enter, and infect cells. *J. Virol.* **75**:3896–3902.
35. Parker, J. S., and C. R. Parrish. 2000. Cellular uptake and infection by canine parvovirus involves rapid dynamin-regulated clathrin-mediated endocytosis, followed by slower intracellular trafficking. *J. Virol.* **74**:1919–1930.
36. Parker, J. S. L., and C. R. Parrish. 1997. Canine parvovirus host range is determined by the specific conformation of an additional region of the capsid. *J. Virol.* **71**:9214–9222.
37. Parrish, C. R. 1991. Mapping specific functions in the capsid structure of canine parvovirus and feline panleukopenia virus using infectious plasmid clones. *Virology* **183**:195–205.
38. Ploubidou, A., V. Moreau, K. Ashman, I. Reckmann, C. Gonzalez, and M. Way. 2000. Vaccinia virus infection disrupts microtubule organization and centrosome function. *EMBO J.* **19**:3932–3944.
39. Pohl, K., and Y. D. Stierhof. 1998. Action of gold chloride (“gold toning”) on silver-enhanced 1 nm gold markers. *Microsc. Res. Tech.* **42**:59–65.
40. Presley, J. F., N. B. Cole, T. A. Schroer, K. Hirschberg, K. J. Zaal, and S. J. Lippincott. 1997. ER-to-Golgi transport visualized in living cells. *Nature* **389**:81–85.
41. Rieddorf, J., A. Ploubidou, I. Reckmann, A. Holmstrom, F. Frischknecht, M. Zettl, T. Zimmermann, and M. Way. 2001. Kinesin-dependent movement on microtubules precedes actin-based motility of vaccinia virus. *Nat. Cell Biol.* **3**:992–1000.
42. Saib, A., M. Neves, M. L. Giron, M. C. Guillemin, J. Valla, J. Peries, and M. Canivet. 1997. Long-term persistent infection of domestic rabbits by the human foamy virus. *Virology* **228**:263–268.
43. Sawada, H., and M. Esaki. 2000. A practical technique to postfix nanogold-immunolabeled specimens with osmium and to embed them in Epon for electron microscopy. *J. Histochem. Cytochem.* **48**:493–498.
44. Seksek, O., J. Biwersi, and A. S. Verkman. 1997. Translational diffusion of macromolecule-sized solutes in cytoplasm and nucleus. *J. Cell Biol.* **138**:131–142.
45. Sodeik, B., M. W. Ebersold, and A. Helenius. 1997. Microtubule-mediated transport of incoming herpes simplex virus 1 capsids to the nucleus. *J. Cell Biol.* **136**:1007–1021.
46. Suikkanen, S., K. Saajjarvi, J. Hirsimaki, O. Valilehto, H. Reunanan, M. Vihinen-Ranta, and M. Vuento. 2002. Role of recycling endosomes and lysosomes in dynein-dependent entry of canine parvovirus. *J. Virol.* **76**:4401–4411.
47. Suomalainen, M., M. Y. Nakano, K. Boucke, S. Keller, and U. F. Greber. 2001. Adenovirus-activated PKA and p38/MAPK pathways boost microtubule-mediated nuclear targeting of virus. *EMBO J.* **20**:1310–1319.
48. Suomalainen, M., M. Y. Nakano, S. Keller, K. Boucke, R. P. Stidwill, and U. F. Greber. 1999. Microtubule-dependent plus- and minus end-directed motilities are competing processes for nuclear targeting of adenovirus. *J. Cell Biol.* **144**:657–672.
49. Tsao, J., S. Chapman, M. Agbandje, W. Keller, K. Smith, H. Wu, M. Luo, T. J. Smith, M. G. Rossman, R. W. Compans, and C. R. Parrish. 1991. The three-dimensional structure of canine parvovirus and its functional implications. *Science* **251**:1456–1464.
50. Valetti, C., D. M. Wetzel, M. Schrader, M. J. Hasbani, S. R. Gill, T. E. Kreis, and T. A. Schroer. 1999. Role of dynein in endocytic traffic: effects of dynamin overexpression and colocalization with CLIP-170. *Mol. Biol. Cell* **10**:4107–4120.
51. Vaughan, P. S., J. D. Leszyk, and K. T. Vaughan. 2001. Cytoplasmic dynein intermediate chain phosphorylation regulates binding to dynein. *J. Biol. Chem.* **276**:26171–26179.
52. Vihinen-Ranta, M., A. Kalela, P. Mäkinen, L. Kakkola, V. Marjomäki, and M. Vuento. 1998. Intracellular route of canine parvovirus entry. *J. Virol.* **72**:802–806.
53. Vihinen-Ranta, M., L. Kakkola, A. Kalela, P. Vilja, and M. Vuento. 1997. Characterization of a nuclear localization signal of canine parvovirus capsid proteins. *Eur. J. Biochem.* **1**:389–394.
54. Vihinen-Ranta, M., D. Wang, W. S. Weichert, and C. R. Parrish. 2002. The VP1 N-terminal sequence of canine parvovirus affects nuclear transport of capsids and efficient cell infection. *J. Virol.* **76**:1884–1891.
55. Vihinen-Ranta, M., W. Yuan, and C. R. Parrish. 2000. Cytoplasmic trafficking of the canine parvovirus capsid and its role in infection and nuclear transport. *J. Virol.* **74**:4853–4859.
56. Weichert, W. S., J. S. L. Parker, A. T. M. Wahid, S.-F. Chang, E. Meier, and C. R. Parrish. 1998. Assaying for structural variation in the parvovirus capsid and its role in infection. *Virology* **250**:106–117.
57. Wikoff, W. R., G. Wang, C. R. Parrish, R. H. Cheng, M. L. Strassheim, T. S. Baker, and M. G. Rossmann. 1994. The structure of a neutralized virus: canine parvovirus complexed with neutralizing antibody fragment. *Structure* **2**:595–607.
58. Xie, Q., and M. S. Chapman. 1996. Canine parvovirus capsid structure, analyzed at 2.9 Å resolution. *J. Mol. Biol.* **264**:497–520.
59. Ye, G. J., K. T. Vaughan, R. B. Vallee, and B. Roizman. 2000. The herpes simplex virus 1 U_L34 protein interacts with a cytoplasmic dynein intermediate chain and targets nuclear membrane. *J. Virol.* **74**:1355–1363.
60. Yeung, D. E., G. W. Brown, P. Tam, R. H. Russnak, G. Wilson, I. Clark-Lewis, and C. R. Astell. 1991. Monoclonal antibodies to the major nonstructural nuclear protein of minute virus of mice. *Virology* **181**:35–45.
61. Yuan, W., and C. R. Parrish. 2000. Comparison of two single-chain antibodies that neutralize canine parvovirus: analysis of an antibody-combining site and mechanisms of neutralization. *Virology* **269**:471–480.